CHAPTER 4

GEOCHEMISTRY

4.1 Sample Preparation

The samples presented in this Chapter are those petrographically described in Chapter 3, which include 13 outcrop samples and 3 core samples of coherent facies of basaltic lavas, 19 core samples of coherent facies of basaltic cobbles and boulders from basalt breccia and 11 core samples of matrix-supported basalt breccia, with pebble-grade clasts (up to 5 mm across). The coherent facies basaltic samples were carefully selected for whole-rock chemical analyses by splitting into conveniently sizes using Rocklabs hydraulic splitter/crusher. These crushed fragments were cautiously chosen to avoid vesicles, amygdale minerals, veinlets, megacrysts and weathered surfaces. The selected chips were blown by compressed air to remove dusty materials. Approximate 50 g aliquots of the cleaned chips were pulverized for a few minutes using a Rocklabs tungsten-carbide ring mill. The core samples of matrix-supported, pebble-grade basalt breccia are largely altered, in particular the matrix portion. They were similarly splitted, crushed and then pulverized, regardless of the altered portions. The powdered samples for basalt breccia had been heated at 1,050 °C for 12 hours before chemical analyses were carried out since they were much more altered than the coherent facies volcanic rocks, resulting in much higher loss on ignition (herein LOI) relative to the rock standards used. All the preparation procedures were done at the Department of Geological Sciences, Faculty of Science, Chiang Mai University.

4.2 Analytical Techniques

4.2.1 Major- and Trace-element Analyses

The powder samples were analyzed for major and minor oxides (SiO_2, TiO_2, Al_2O_3, total iron as Fe_2O_3, MnO, MgO, CaO, Na_2O, K_2O, P_2O_5 and LOI), and trace elements (Ba, Rb, Sr, Y, Zr, V, Ni, Nb, Th, Sc and Cr). All the analyses of major and minor oxides, and trace elements were carried out at the Department of Geological Sciences, Faculty of Science, Chiang Mai University.

Most of the analyses for major and minor oxides (excluding LOI) and trace elements were obtained using a Phillips Magic Pro Wavelength Dispersive X-ray Fluorescence (XRF) Spectrometer with PW1510 Sample Changer. The instrumental parameters are made up of (1) Rhodium (Rh) tube with a lithium fluoride 200 crystal (used in an elemental range of K – Ru, and scintillation and flow proportion detectors, and (2) X-ray tube operated at 60 kV and current of up to 125 mA at a maximum power level of 4 kW. The net (background corrected) intensities were measured and the concentrations were calculated against the calibrations derived from 5 international standard reference materials (AGV-2, BCR-2, BHVO-2, BIR-1 and RGM-1). The inter-elements matrix corrections were done by the Super Q version 3.0 program. The reporting detection limits are about 0.01 wt% for major oxides and 3 ppm for trace elements. The accuracy and precision for most elements are better than 5%.

Major oxides were measured from fusion discs prepared with 0.06 g lithium bromide (LiBr), 3 g Lithium Tetra Borate ($Li_2B_4O_4$) and 0.6 g sample powder. Trace elements were performed on pellets made from pressed sample powder. These were prepared using 5 g of sample powder with approximately 0.3 g wax ($C_6H_8O_3N_2$) which had been mixed with boric acid (H_3BO_3) in aluminium cup prior to pressing. Several international standard samples, including AGV-2, BCR-2, BHVO-2, BIR-1 and RGM-1, were measured during XRF analysis.

Ignition loss was gravimetrically determined by the author at the Department of Geological Sciences, Faculty of Science, Chiang Mai University via heating approximately 1.0 g of powdered sample at 1,050 °C for 12 hours.

4.2.2 REE and Hf, Ta Analysis

Eight representatives of these samples were analyzed for rare-earth elements (herein REE) (La, Ce, Pr, Nd, Sm, Eu, Gd, Tb, Dy, Ho, Er, Tm and Yb), Ta and Hf. Analyses were done using ICP-MS (Inductively Coupled Plasma - Mass Spectrometry) installed at the School of Earth Sciences, Royal Holloway College, University of London. The solutions for ICP-MS analysis were prepared and analyzed by Dr. John Nicholas Walsh, Department of Earth Sciences, Royal Holloway College, University of London (Walsh *et al.,* 1981).

The sample preparation for REE analysis has been carried out using the procedures as follows:

(1) Weigh 0.5 g of pulverized rock samples and 1 standard into platinum crucibles. Add 12 ml of HF and $HClO_4$ mixture from the dispenser to a batch of 1 blank, 1 standard and a number of rock samples. Digest each batch to dryness on a sand bath (no $HClO_4$ remains). When the crucibles are no longer fuming, remove them from the sand bath and allow cool. Add 5ml of HCl and a little distilled water to each sample, and put back on the sand bath to warm for 5 minutes. Then add more distilled water till each crucible is 3/4 full and warm for a further 15 minutes or until dissolved. Remove crucibles and allow cool.

(2) Filter each crucible into a 100 ml beaker, using a number 42 ashless filter paper. Rinse each filter paper several times with distilled water, but do not let the filtrate exceed 60ml. Clean silver crucibles by immersing them in HCl and then rinsing with distilled water. Fold the filter papers into each crucible and put them into the furnace. Heat the crucibles to 800°C with 200°C increments and leave for 30 minutes at 800°C. Remove the crucibles from the furnace, using long-handled tongs, allow them to cool, and then add 6 pellets of sodium hydroxide to each sample. Put them back into the furnace for another 30 minutes at 800°C. Remove

each crucible separately, swirling the mixture until it solidifies. Allow to cool and then half fill each crucible with distilled water. Leave for 30 minutes to digest the fusion cake and then add 5 ml of HCl to each silver crucible. Add the fusion portion to the filtered portion of each sample and make them up to approximately 100 ml with distilled water. Wash the silver crucibles with warm water and store them in a beaker of distilled water.

(3) Make 1.7 M HCl, by adding 600 ml HCl to 3400 ml distilled water, and 4.0M HCl, by adding 1700 ml HCl to 3100 ml of distilled water. Using a graduated cylinder, put 500 ml of 1.7M HCl into each round bottomed flask. Place a clean labelled 800 ml beaker under each column. Drain each column, and then load on the samples, rinsing the beakers onto the columns. When all samples have passed through, elute the columns with 500 ml of 1.7M HCl, to remove the major and trace elements from the resin. Discard this portion when all the 1.7M HCl has run through. Wash funnel and beaker with distilled water, and elute the columns with 600 ml of 4.0M HCl, saving the eluted portion. Evaporate on a hotplate until approximately 15 ml remains, and then transfer to a 50ml beaker, rinsing it in with distilled water and take down to dryness. Cool and cover beaker with a cling film. After using the columns, rinse them with 200 ml of 5% HCl. Turn off the columns leaving a little 5% HCl on top of the resin.

(4) Before running the representative samples on the ICP-MS, punch a small hole in the cling film and add 5 ml of 10% HNO_3 through the hole. Then place 4 beakers at a time in the microwave and heat for 13 seconds on power 10. Allow to cool and then transfer to small washed tubes. The samples are now ready to analyze on the ICP-MS.

4.3 Magmatic Affinities and Rock Types

The studied samples of coherent facies basaltic lavas from outcrops and drill cores, coherent facies cobble- and boulder-grade basaltic clasts from basalt breccia, and the matrix-supported basalt breccia have narrow compositional ranges and incompatible-element ratios (Tables 4.1 and 4.2). The basaltic samples from coherent facies basaltic lavas and the basaltic clasts in basalt breccia have similar chemical

Table 4.1 Major oxides (wt%), normalized to 100 wt% on the basis of LOI free, and CIPW norms of the coherent facies basaltic lavas, coherent facies basaltic clasts in basalt breccia and the matrix-supported basalt breccia from Ban Sap Sawat, Wichian Buri District, Phetchabun Province. Also reported are original sum, LOI and mg#.

Sample no.	Major oxides (wt.%)											Original Sum	LOI	mg#	CIPW norms (%)																			
	SiO_2	TiO_2	Al_2O_3	Fe_2O_3	FeO	MnO	MgO	CaO	Na_2O	K_2O	P_2O_5				Qtz	Or	Ab	An	Ne	C	Di (wo)	Di (en)	Di (fs)	Hy (en)	Hy (fs)	Ol (fo)	Ol (fa)	Mt	He	Il	Ap
Coherent facies basaltic lavas (outcrop samples)																																		
WB-1	47.54	1.56	16.57	1.88	10.43	0.15	8.01	9.34	3.53	0.71	0.28	100.07	0.64	0.37	0	4.20	24.22	27.23	3.04	0	7.30	3.99	3.04	0	0	11.23	9.45	2.73	0	2.96	0.61
WB-2	47.75	1.61	16.58	1.86	10.33	0.16	7.82	9.41	3.50	0.71	0.28	100.50	1.02	0.37	0	4.20	24.94	27.39	2.51	0	7.37	4.02	3.09	0	0	10.87	9.24	2.70	0	3.06	0.61
WB-3	47.67	1.55	16.86	1.85	10.27	0.15	8.07	9.30	3.34	0.66	0.28	100.31	1.24	0.38	0	3.90	25.47	29.02	1.50	0	6.47	3.56	2.65	0	0	11.63	9.56	2.68	0	2.95	0.61
WB-4	48.19	1.53	17.10	1.78	9.89	0.14	7.96	9.06	3.42	0.66	0.28	100.65	1.64	0.38	0	3.90	27.53	29.32	0.75	0	5.85	3.26	2.36	0	0	11.65	9.31	2.58	0	2.91	0.61
WB-5	47.87	1.54	16.96	1.82	10.11	0.14	7.96	9.07	3.55	0.69	0.29	99.98	0.79	0.38	0	4.08	26.11	28.27	2.11	0	6.28	3.47	2.57	0	0	11.50	9.41	2.64	0	2.93	0.63
WB-6	47.26	1.58	17.37	1.77	9.84	0.14	8.26	9.72	3.14	0.63	0.30	100.33	1.23	0.39	0	3.73	23.80	31.40	1.48	0	6.30	3.57	2.46	0	0	11.96	9.10	2.57	0	3.00	0.65
WB-7	46.98	1.53	17.43	1.81	10.05	0.14	8.29	9.74	3.20	0.54	0.30	100.16	1.45	0.39	0	3.19	23.31	31.56	2.02	0	6.27	3.52	2.49	0	0	12.04	9.41	2.62	0	2.91	0.65
WB-8	46.58	1.47	17.44	1.82	10.10	0.14	8.71	9.82	3.09	0.56	0.28	100.16	1.35	0.40	0	3.31	21.49	32.02	2.51	0	6.29	3.58	2.44	0	0	12.74	9.59	2.64	0	2.79	0.61
WB-9	48.12	1.55	16.76	1.82	10.12	0.14	7.86	9.15	3.53	0.67	0.28	100.55	1.13	0.38	0	3.96	26.84	27.87	1.62	0	6.64	3.65	2.74	0	0	11.20	9.28	2.64	0	2.95	0.61
WB-10	47.21	1.38	17.27	1.82	10.11	0.14	8.46	9.63	3.27	0.48	0.24	100.30	1.10	0.39	0	2.84	23.84	30.98	2.06	0	6.43	3.60	2.56	0	0	12.28	9.63	2.64	0	2.62	0.52
WB-11	47.18	1.54	17.23	1.78	9.91	0.14	8.20	9.67	3.45	0.62	0.29	100.55	1.05	0.39	0	3.67	22.95	29.65	3.36	0	6.94	3.91	2.75	0	0	11.61	9.02	2.58	0	2.93	0.63
WB-12	47.38	1.44	17.35	1.79	9.93	0.14	8.18	9.87	3.18	0.47	0.27	100.66	1.05	0.39	0	2.78	24.47	31.64	1.31	0	6.58	3.68	2.63	0	0	11.74	9.26	2.60	0	2.74	0.59
WB-13	47.47	1.43	17.21	1.82	10.12	0.15	7.46	9.39	3.93	0.56	0.45	99.59	1.71	0.36	0	3.31	25.12	27.63	4.39	0	6.82	3.66	2.93	0	0	10.50	9.30	2.64	0	2.72	0.98
Coherent facies basaltic lavas (core samples)																																		
WB-27	47.43	1.41	17.44	1.76	9.79	0.14	8.02	9.70	3.49	0.53	0.29	99.85	0.81	0.39	0	3.13	24.11	30.32	2.92	0	6.73	3.76	2.70	0	0	11.41	9.06	2.55	0	2.68	0.63
WB-30	47.92	1.30	16.98	1.75	9.72	0.15	8.45	8.72	3.93	0.77	0.31	100.14	1.39	0.40	0	4.55	25.02	26.38	4.44	0	6.30	3.57	2.45	0	0	12.29	9.32	2.54	0	2.47	0.68
WB-36	47.82	1.30	17.29	1.73	9.62	0.15	8.52	9.59	3.07	0.60	0.31	99.63	2.07	0.41	0	3.55	25.54	31.58	0.22	0	5.93	3.38	2.28	0	0	12.54	9.32	2.51	0	2.47	0.68

LOI = Loss on ignition; mg # = molecular MgO/(MgO+FeO); and FeO and Fe_2O_3 were calculated using Fe_2O_3/FeO=0.2 (Middlemost, 1989).

Table 4.1 (Continued)

Sample no.	Major oxides (wt%)											Original Sum	LOI	mg#	CIPW norms (%)																		
	SiO_2	TiO_2	Al_2O_3	Fe_2O_3	FeO	MnO	MgO	CaO	Na_2O	K_2O	P_2O_5				Qtz	Or	Ab	An	Ne	C	Di (wo)	Di (en)	Di (fs)	Hy (en)	Hy (fs)	Ol (fo)	Ol (fa)	Mt	He	Il	Ap
Coherent facies basaltic clasts in basalt breccia (core samples)																																	
WB-14	46.37	1.46	17.43	1.78	9.92	0.14	8.58	10.34	3.33	0.36	0.29	100.19	1.66	0.40	0	2.13	20.38	31.51	4.21	0	7.56	4.30	2.92	0	0	12.00	9.00	2.58	0	2.77	0.63
WB-17	47.53	1.26	17.42	1.72	9.57	0.14	8.48	9.90	3.27	0.43	0.27	100.69	1.22	0.41	0	2.54	24.33	31.55	1.80	0	6.68	3.81	2.57	0	0	12.17	9.07	2.49	0	2.39	0.59
WB-19	47.83	1.27	17.12	1.74	9.67	0.15	8.61	9.53	3.30	0.49	0.28	101.08	1.86	0.41	0	2.90	25.66	30.42	1.21	0	6.36	3.63	2.44	0	0	12.52	9.30	2.52	0	2.41	0.61
WB-21	48.08	1.27	17.23	1.72	9.54	0.15	8.42	9.73	3.06	0.51	0.31	100.23	1.06	0.41	0	3.02	25.86	31.72	0	0	6.15	3.51	2.37	0.73	0.50	11.77	8.80	2.49	0	2.41	0.68
WB-22	48.37	1.23	17.23	1.70	9.48	0.14	8.25	8.82	3.70	0.78	0.29	99.88	1.44	0.40	0	4.67	26.46	28.03	2.61	0	5.86	3.32	2.29	0	0	12.11	9.21	2.47	0	2.34	0.63
WB-25	48.38	1.27	17.17	1.71	9.53	0.14	8.42	8.43	3.87	0.78	0.31	100.49	2.58	0.41	0	4.61	27.22	27.13	2.97	0	5.38	3.07	2.07	0	0	12.59	9.39	2.48	0	2.41	0.68
WB-29	48.12	1.26	17.03	1.73	9.60	0.14	8.39	9.08	3.53	0.82	0.30	100.76	2.26	0.40	0	4.85	25.18	28.16	2.52	0	6.32	3.59	2.46	0	0	12.17	9.19	2.51	0	2.39	0.65
WB-32	47.42	1.25	17.29	1.76	9.78	0.14	8.60	9.43	3.40	0.61	0.32	99.98	1.94	0.41	0	3.61	23.85	30.07	2.65	0	6.20	3.52	2.40	0	0	12.58	9.48	2.55	0	2.38	0.70
WB-34	47.57	1.25	17.32	1.72	9.59	0.13	8.54	9.53	3.43	0.60	0.32	100.31	2.07	0.41	0	3.55	24.06	30.05	2.67	0	6.42	3.67	2.46	0	0	12.38	9.18	2.49	0	2.38	0.70
WB-35	48.01	1.26	17.27	1.70	9.46	0.14	8.30	9.34	3.60	0.61	0.31	99.98	1.76	0.40	0	3.61	25.56	29.12	2.64	0	6.44	3.66	2.49	0	0	11.96	8.99	2.47	0	2.39	0.68
WB-38	48.25	1.25	17.22	1.73	9.60	0.14	8.21	9.30	3.48	0.51	0.31	100.09	2.56	0.40	0	3.02	27.43	29.82	1.07	0	6.06	3.41	2.39	0	0	11.98	9.26	2.51	0	2.38	0.68
WB-40	47.66	1.58	17.29	1.83	10.19	0.15	7.99	9.21	3.03	0.79	0.29	100.60	4.22	0.38	0	4.67	25.61	31.20	0	0	5.35	2.95	2.19	0.12	0.09	11.83	9.71	2.65	0	3.00	0.63
WB-41	47.66	1.49	17.13	1.83	10.17	0.14	7.79	9.38	3.50	0.60	0.30	100.18	2.35	0.37	0	3.55	25.49	29.22	2.21	0	6.52	3.56	2.73	0	0	11.14	9.43	2.65	0	2.83	0.65
WB-42	47.55	1.56	17.16	1.81	10.05	0.14	7.70	10.06	3.23	0.46	0.29	99.79	1.64	0.37	0	2.72	25.07	30.92	1.20	0	7.22	3.95	3.00	0	0	10.71	8.98	2.62	0	2.96	0.63
WB-43	46.90	1.53	17.31	1.79	9.93	0.14	8.24	10.09	3.36	0.43	0.29	99.86	1.28	0.39	0	2.54	22.46	30.84	3.21	0	7.32	4.12	2.89	0	0	11.53	8.94	2.60	0	2.91	0.63
WB-44	47.20	1.54	17.31	1.74	9.65	0.14	8.31	10.17	3.24	0.41	0.29	100.50	1.49	0.40	0	2.43	23.50	31.44	2.10	0	7.24	4.13	2.78	0	0	11.65	8.65	2.52	0	2.93	0.63
WB-46	46.96	1.44	17.27	1.83	10.16	0.14	8.48	9.39	3.70	0.34	0.28	100.22	2.39	0.39	0	2.01	23.97	29.47	3.95	0	6.47	3.63	2.57	0	0	12.32	9.61	2.65	0	2.74	0.61
WB-47	47.06	1.40	17.68	1.72	9.58	0.14	8.43	10.05	3.35	0.31	0.28	100.13	0.55	0.41	0	1.83	23.50	32.25	2.61	0	6.68	3.82	2.55	0	0	12.08	8.92	2.49	0	2.66	0.61
WB-49	48.27	1.24	17.18	1.74	9.68	0.14	8.40	8.67	3.60	0.78	0.29	100.19	1.73	0.40	0	4.61	26.79	28.38	1.97	0	5.41	3.06	2.12	0	0	12.56	9.59	2.52	0	2.36	0.63

LOI = Loss on ignition; mg # = molecular MgO/(MgO+FeO); and FeO and Fe_2O_3 were calculated using Fe_2O_3/FeO=0.2 (Middlemost, 1989).

Table 4.1 (Continued)

Sample no.	Major oxides (wt%)											Original Sum	LOI	mg#	CIPW norms (%)																
	SiO_2	TiO_2	Al_2O_3	Fe_2O_3	FeO	MnO	MgO	CaO	Na_2O	K_2O	P_2O_5				Qtz	Or	Ab	An	Ne	C	Di (wo)	Di (en)	Di (fs)	Hy (en)	Hy (fs)	Ol (fo)	Ol (fa)	Mt	He	Il	Ap
Matrix - supported basalt breccia (core samples)																															
WB-15	47.37	1.39	17.30	1.77	9.82	0.14	8.65	10.04	2.62	0.63	0.29	99.61	9.80	0.41	0	3.73	22.14	33.53	0	0	6.09	3.48	2.34	1.67	1.12	11.53	8.54	2.57	0	2.64	0.63
WB-16	47.88	1.41	17.17	1.76	9.77	0.14	8.53	9.80	2.71	0.53	0.29	100.89	8.13	0.40	0	3.14	22.91	33.08	0	0	5.79	3.30	2.23	3.70	2.50	10.03	7.47	2.55	0	2.68	0.63
WB-18	48.84	1.26	17.08	1.72	9.59	0.15	8.68	8.99	2.73	0.70	0.28	100.81	8.56	0.41	0	4.14	23.07	32.23	0	0	4.48	2.57	1.70	6.97	4.61	8.51	6.22	2.49	0	2.39	0.61
WB-20	48.65	1.24	17.28	1.70	9.46	0.14	8.61	8.96	2.84	0.81	0.31	99.76	8.33	0.41	0	4.79	24.00	31.97	0	0	4.46	2.57	1.69	4.72	3.11	9.96	7.23	2.47	0	2.36	0.68
WB-24	48.69	1.28	17.85	1.67	9.28	0.14	8.55	9.09	2.38	0.75	0.31	100.17	9.70	0.42	0	4.44	20.12	35.76	0	0	3.15	1.82	1.18	10.25	6.61	6.52	4.64	2.42	0	2.43	0.68
WB-26	48.98	1.29	17.31	1.76	9.81	0.15	10.27	7.43	1.95	0.73	0.32	100.12	12.76	0.45	0	4.32	16.48	35.01	0	0.47	0	0	0	20.26	11.59	3.79	2.39	2.55	0	2.45	0.70
WB-28	48.04	1.25	17.18	1.76	9.81	0.14	8.38	9.34	3.34	0.47	0.31	99.81	7.26	0.40	0	2.78	27.16	30.45	0.58	0	5.88	3.31	2.32	0.00	0.00	12.35	9.57	2.55	0	2.37	0.68
WB-31	48.91	1.26	16.72	1.74	9.65	0.16	8.56	9.29	2.63	0.76	0.31	100.79	8.71	0.41	0	4.50	22.23	31.53	0	0	5.33	3.04	2.05	7.22	4.88	7.80	5.83	2.52	0	2.39	0.68
WB-33	48.80	1.23	16.95	1.70	9.44	0.13	8.40	9.37	2.90	0.76	0.30	99.40	11.29	0.41	0	4.50	24.51	30.95	0	0	5.76	3.29	2.21	3.79	2.55	9.75	7.23	2.47	0	2.34	0.66
WB-37	48.59	1.25	17.07	1.69	9.39	0.14	8.42	9.68	2.85	0.61	0.32	99.55	9.43	0.41	0	3.61	24.08	31.94	0	0	5.94	3.40	2.27	4.01	2.67	9.55	7.02	2.45	0	2.37	0.70
WB-39	48.75	1.56	17.68	1.80	10.03	0.14	9.92	7.60	1.35	0.86	0.29	101.11	19.24	0.43	0.56	5.09	11.41	36.03	0	1.31	0	0	0	24.80	14.59	0	0	2.61	0	2.96	0.63

LOI = Loss on ignition; mg # = molecular MgO/(MgO+FeO); and FeO and Fe_2O_3 were calculated using Fe_2O_3/FeO=0.2 (Middlemost, 1989).

Table 4.2 Trace elements content (ppm) and some selected incompatible-element ratios for coherent facies basaltic lavas, coherent facies basaltic clasts in basalt breccia and matrix-supported basalt breccia from Ban Sap Sawat, Wichian Buri District, Phetchabun Province

Sample no.	Trace elements content (ppm) and some selected ratios																			
	Ba	Rb	Th	Sr	Nb	Zr	Y	Cr	Ni	V	Sc	Ti/Zr	P/Zr	K/Ba	Zr/Nb	Zr/Y	Ti/Y	Ti/V	Sr/Rb	Ba/Rb	Th/Nb
Coherent facies basaltic lavas (outcrop samples)																				
WB-1	285	10	9	527	8	141	33	369	115	242	28	66	8.7	21	18	4.2	281	39	54	29	1.1
WB-2	274	11	7	508	8	141	34	336	121	251	35	69	8.7	22	18	4.1	284	39	47	26	0.9
WB-3	267	10	6	534	8	142	33	351	127	243	27	65	8.6	21	18	4.3	284	38	55	27	0.8
WB-4	206	8	5	543	8	141	21	273	99	184	25	65	8.7	27	18	6.8	443	50	65	25	0.6
WB-5	290	12	7	537	8	144	33	330	117	237	30	64	8.8	20	18	4.3	276	39	47	25	0.8
WB-6	212	8	4	589	8	149	23	262	97	185	22	64	8.8	25	19	6.4	404	51	75	27	0.5
WB-7	273	9	6	618	8	151	35	341	139	246	33	61	8.6	16	19	4.4	265	37	71	31	0.7
WB-8	264	8	7	592	6	144	33	350	145	232	26	61	8.5	18	22	4.3	263	38	76	34	1.2
WB-9	271	11	6	554	8	143	33	341	122	246	34	65	8.6	21	18	4.4	286	38	52	26	0.7
WB-10	219	9	6	542	4	138	35	345	153	232	32	60	7.6	18	33	4.0	238	36	62	25	1.4
WB-11	206	8	5	567	8	145	23	241	100	182	20	64	8.7	25	18	6.4	409	51	75	27	0.7
WB-12	232	8	6	610	4	141	35	339	133	232	31	61	8.4	17	32	4.1	250	37	73	28	1.5
WB-13	231	7	6	658	7	157	24	207	79	179	16	55	12.5	20	21	6.6	357	48	93	33	0.8
Coherent facies basaltic lavas (core samples)																				
WB-27	244	9	7	580	4	142	35	313	134	235	32	60	8.9	18	33	4.0	239	36	63	27	1.7
WB-30	295	12	6	517	8	150	36	365	172	212	33	52	9.0	22	19	4.1	215	37	43	25	0.7
WB-36	276	10	7	491	8	149	36	359	163	228	31	52	9.1	18	18	4.1	216	34	50	28	0.8

Table 4.2 (Continued)

Sample no.	Trace elements content (ppm) and some selected ratios																			
	Ba	Rb	Th	Sr	Nb	Zr	Y	Cr	Ni	V	Sc	Ti/Zr	P/Zr	K/Ba	Zr/Nb	Zr/Y	Ti/Y	Ti/V	Sr/Rb	Ba/Rb	Th/Nb
Coherent facies basaltic clasts in basalt breccia (core samples)																				
WB-14	266	6	7	619	4	147	36	331	140	251	34	60	8.6	11	33	4.0	241	35	95	41	1.5
WB-17	283	8	8	485	6	143	36	361	158	223	33	53	8.3	13	22	4.0	211	34	64	38	1.2
WB-19	260	8	6	475	7	142	35	366	167	228	32	54	8.6	16	22	4.1	220	33	56	31	1.0
WB-21	269	8	7	508	8	149	37	364	165	226	31	51	9.1	16	20	4.0	205	34	66	35	0.9
WB-22	296	9	7	535	8	149	34	350	168	219	31	49	8.5	22	20	4.4	215	34	57	32	0.9
WB-25	277	12	6	464	9	146	36	356	176	226	26	52	9.2	23	17	4.1	212	34	40	24	0.7
WB-29	290	10	6	639	7	157	37	356	168	212	35	48	8.3	23	22	4.3	206	36	63	29	0.9
WB-32	288	9	6	517	8	149	36	364	173	225	35	50	9.3	18	19	4.2	208	33	58	32	0.8
WB-34	305	10	6	509	7	150	35	369	168	224	39	50	9.3	16	20	4.2	212	34	53	32	0.8
WB-35	280	9	7	505	7	149	37	364	167	222	37	51	9.1	18	20	4.0	206	34	55	30	0.9
WB-38	260	7	7	507	8	149	37	363	175	220	32	50	9.1	16	20	4.0	203	34	68	35	0.9
WB-40	261	10	6	604	8	146	31	315	122	242	25	65	8.6	25	17	4.8	310	39	58	25	0.7
WB-41	215	7	5	503	8	142	23	241	94	187	26	63	9.2	23	18	6.1	386	48	73	31	0.7
WB-42	267	8	7	516	8	140	33	324	115	253	33	67	9.0	14	17	4.3	285	37	62	32	0.8
WB-43	283	7	6	572	7	147	35	338	140	254	32	62	8.6	13	20	4.2	263	36	82	40	0.8
WB-44	267	7	7	582	8	146	34	334	139	259	38	63	8.6	13	19	4.3	274	36	85	39	0.9
WB-46	203	6	5	576	6	145	25	264	114	190	25	60	8.4	14	25	5.9	350	46	99	35	0.9
WB-47	246	6	7	583	5	143	37	334	143	247	39	59	8.6	10	27	3.8	226	34	104	44	1.2
WB-49	280	10	8	618	8	155	37	362	165	220	34	48	8.2	23	19	4.2	199	34	60	27	1.0

Table 4.2 (Continued)

Sample no.	Trace elements content (ppm) and some selected ratios																			
	Ba	Rb	Th	Sr	Nb	Zr	Y	Cr	Ni	V	Sc	Ti/Zr	P/Zr	K/Ba	Zr/Nb	Zr/Y	Ti/Y	Ti/V	Sr/Rb	Ba/Rb	Th/Nb
Matrix-supported basalt breccias (core samples)																				
WB-15	269	9	6	616	5	144	34	331	147	232	36	58	8.8	19	30	4.3	247	36	65	28	1.2
WB-16	245	9	6	664	5	148	34	336	134	236	35	57	8.5	18	31	4.3	248	36	74	27	1.4
WB-18	252	12	7	504	7	144	35	368	161	223	41	52	8.5	23	21	4.1	214	34	44	22	1.0
WB-20	286	13	7	522	8	149	36	361	166	223	35	50	9.1	24	19	4.2	208	33	40	22	1.0
WB-24	295	11	6	532	9	153	36	352	155	219	40	50	8.9	21	18	4.2	211	35	47	26	0.7
WB-26	325	14	7	601	7	158	37	355	157	244	39	49	8.8	19	21	4.2	207	32	43	23	0.9
WB-28	261	10	7	455	7	145	36	353	150	235	38	52	9.4	15	20	4.0	207	32	47	27	0.9
WB-31	269	12	7	643	8	156	35	346	151	230	42	48	8.7	23	21	4.4	215	33	52	22	0.9
WB-33	287	12	7	575	8	150	35	352	157	222	33	49	8.7	22	19	4.3	212	33	46	23	0.9
WB-37	247	10	7	608	8	154	34	349	157	217	34	49	9.1	21	19	4.5	219	34	61	25	0.8
WB-39	342	14	7	603	8	144	33	304	119	258	33	65	8.8	21	17	4.3	281	36	44	25	0.9

compositions (Table 4.3), implying that they are essentially co-magmatic. Although the matrix-supported basalt brecia samples have partially experienced alteration, as illustrated by their modally modified constituents and relatively high LOI content (7.26 – 19.24 wt%), their chemical compositions are insignificantly different from the coherent facies basaltic rocks (Table 4.3), but for Na_2O of the matrix-supported basalt breccia samples (2.57 ± 0.53 wt%) that are slightly lower than those for coherent facies rocks (3.41 ± 0.26 wt% for coherent facies basaltic lavas and 3.42 ± 0.22 wt% for basaltic clasts in basalt breccia).

The primary compositions of the Ban Sap Sawat basaltic rocks, inferred from the geochemical data for coherent facies basaltic lavas and coherent facies basaltic clasts from basalt breccia, are as follows: 47.59 ± 0.50 wt% SiO_2, 1.42 ± 0.13 wt% TiO_2, 17.20 ± 0.24 wt% Al_2O_3, 1.78 ± 0.05 wt% Fe_2O_3, 9.87 ± 0.27 wt% FeO, 0.14 ± 0.01 wt% MnO, 8.24 ± 0.29 wt% MgO, 9.48 ± 0.44 wt% CaO, 3.24 ± 0.23 wt% Na_2O, 0.59 ± 0.14 wt% K_2O, 0.30 ± 0.03 wt% P_2O_5, 261 ± 29 ppm Ba, 8.7 ± 1.7 ppm Rb, 6.3 ± 0.9 ppm Th, 551 ± 50 ppm Sr, 7.2 ± 1.3 ppm Nb, 146 ± 4.8 ppm Zr, 33 ± 4.8 ppm Y, 331 ± 42 ppm Cr, 139 ± 27 ppm Ni, 226 ± 22.5 ppm V, and 30.6 ± 5.2 ppm Sc. The coherent facies basaltic rocks form a compositional field straddling the demarcation line separating an alkalic field from a subalkalic field and are located in the filed of basalt on a total alkalis-silica diagram (Figure 4.1). The coherent facies basaltic lavas and basaltic clasts from basalt breccia, have K_2O/Na_2O ratios varying from 0.09 to 0.26, with an average value of 0.17 ± 0.04. The high K_2O/Na_2O ratios (>0.21) might have been due to alteration, as shown by the higher K_2O/Na_2O values for the matrix-supported basalt breccia (0.14 to 0.64, 0.29 ± 0.13 on average). The transitional subalkalic-alkalic nature is supported by their Nb/Y ratios (0.12 - 0.38, 0.23 ± 0.06 on average) in the limit of subalkalic rocks (Pearce and Cann, 1973; Floyd and Winchester, 1975; Winchester and Floyd, 1977; Pearce, 1982) (Figure 4.2), but their normative nepheline abundances are up to 4.44 wt% (Table 4.1), characteristic of mildly alkalic rocks. The abundances of SiO_2 and total iron as FeO (herein FeO*), and FeO*/MgO ratios (Figure 4.3) signify that the coherent facies basaltic rocks are transitional tholeiite to alkalic basalts rather than transitional calc-alkalic to alkalic basalts.

Table 4.3 Compositional ranges and their averaged values for coherent facies basaltic lava, coherent facies basaltic clasts in basalt breccia, and matrix-supported basalt breccia, The values for major and minor oxides are normalized to 100 wt% on the basis of volatile free.

Major and Minor oxides (wt.%)	Coherent facies basaltic lavas (16 samples)		Cohrent facies basaltic clasts in basalt breccia (19 samples)		Matrix-supported basalt breccia (11 samples)	
	Ranges	Average	Ranges	Average	Ranges	Average
SiO_2	46.58-48.19	(47.52±0.43)	46.37-48.38	(47.64±0.56)	47.37-48.98	(48.50±0.51)
TiO_2	1.30-1.61	(1.48±0.10)	1.23-1.58	(1.36±0.13)	1.23-1.56	(1.31±0.10)
Al_2O_3	16.57-17.44	(17.12±0.30)	17.03-17.68	(17.27±0.14)	16.72-17.85	(17.24±0.32)
Fe_2O_3	1.73-1.88	(1.80 ±0.22)	1.70-1.83	(1.75±0.25)	1.67-1.80	(1.73±0.23)
FeO	9.62-10.43	(10.02±0.04)	9.46-10.19	(9.74±0.05)	9.28-10.03	(9.64±0.04)
MnO	0.14-0.16	(0.14 ±0.01)	0.13-0.15	(0.14±0.01)	0.13-0.16	(0.14±0.01)
MgO	7.46-8.71	(8.14 ±0.31)	7.70-8.61	(8.32±0.26)	8.38-10.27	(8.82±0.65)
CaO	8.72-9.87	(9.45±0.33)	8.43-10.34	(9.50±0.53)	7.43-10.04	(9.05±0.83)
Na_2O	3.07-3.93	(3.41±0.26)	3.03-3.87	(3.42±0.22)	1.35-3.34	(2.57±0.53)
K_2O	0.47-0.77	(0.62±0.09)	0.31-0.82	(0.56±0.17)	0.47-0.86	(0.69±0.12)
P_2O_5	0.24-0.45	(0.30±0.04)	0.27-0.32	(0.30±0.01)	0.28-0.32	(0.30±0.01)
Trace elements (ppm)						
Ba	206-295	(253±31.0)	203-305	(268± 25.3)	245-342	(280±31)
Rb	7-12	(9.2±1.5)	6-12	(8.3±1.7)	9-14	(11.5±1.8)
Th	4-9	(6.2±1.1)	5-8	(6.4±0.7)	6-7	(6.8±0.5)
Sr	491-658	(560±45)	464-639	(543±54)	455-664	(575±64)
Nb	4--8	(7.1±1.5)	4-9	(7.2±1.1)	5-9	(7.2±1.3)
Zr	138-157	145±5.1)	140-157	(147±4.4)	144-158	(150±5.1)
Y	21-36	(31.4±5.3)	23-37	(34.2±4.0)	33-37	(35.1±1.2)
Cr	207-369	(320±48)	241-369	(340±35)	304-368	(346±17)
Ni	79-172	(126±25)	94-176	(150±24)	119-166	(150.4±13.19)
V	179-251	(223±26)	187-259	(228±20)	217-258	(231±12)
Sc	16-35	(28±5)	25-39	(33±4)	33-42	(37±3)

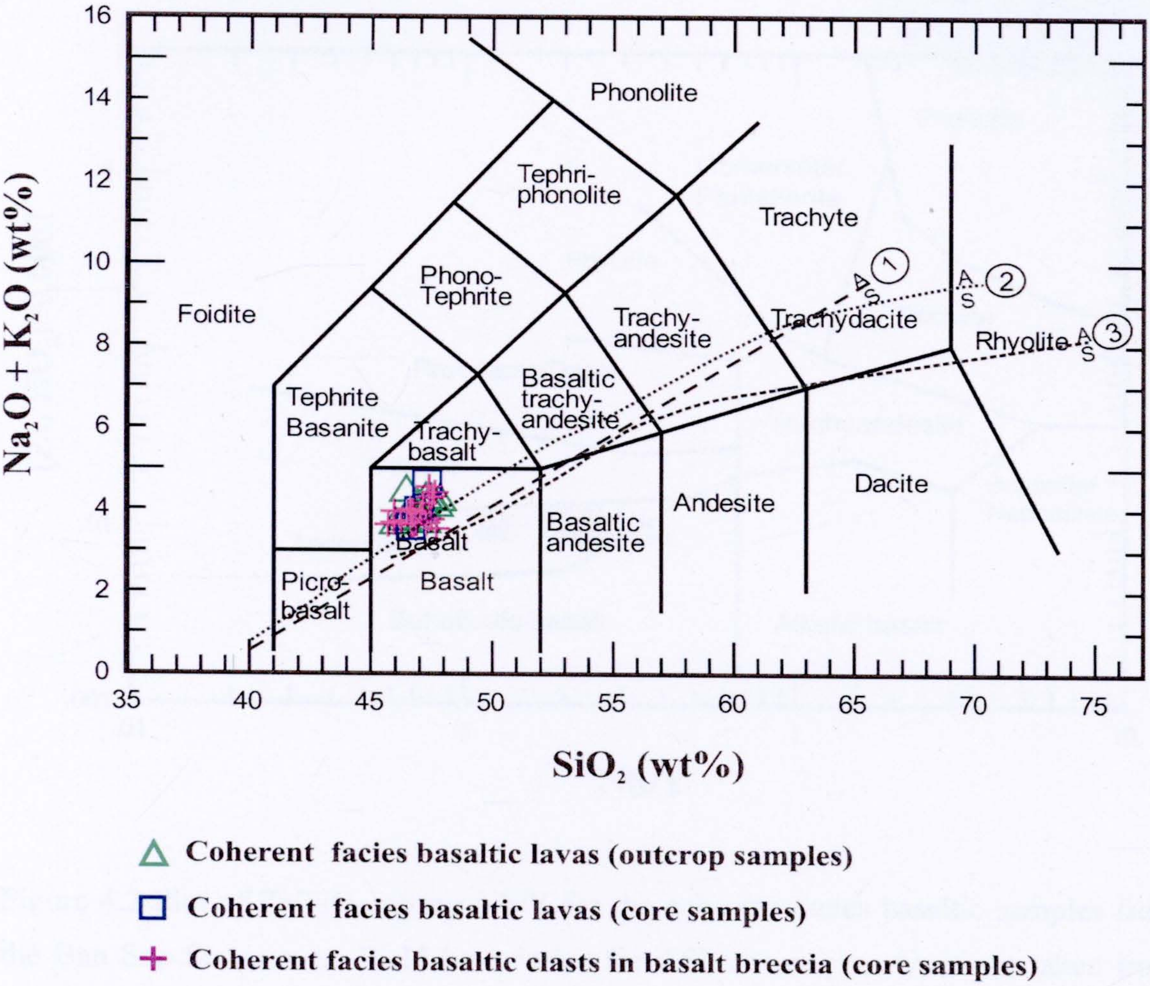

Figure 4.1 Total alkali *versus* silica plot for the Ban Sap Sap Sawat coherent facies basaltic rocks, Delimited fields for different rock types are after Le Bas *et al*., (1986). Also shown are the field boundaries between alkalic series (A) and subalkalic series (S) of (1) MacDonald (1968), (2) Irvine and Baragar (1971), and (3) Kuno (1966).

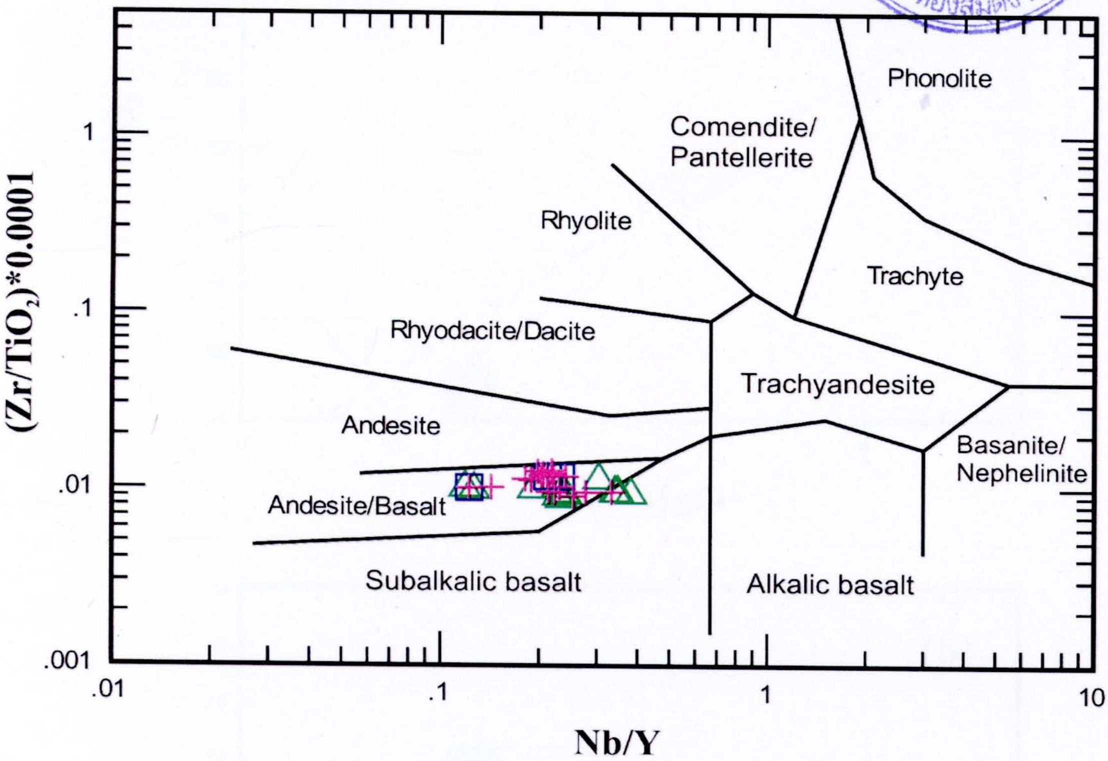

Figure 4.2 Plot of Zr/TiO_2 *versus* Nb/Y for the coherent facies basaltic samples from the Ban Sap Sawat area, Field boundaries for different magma types are taken from Winchester and Floyd (1977). Symbols are as in Figure 4.1.

The proportions of FeO and MgO for the coherent rocks correspond to Mg/(Mg + Fe) (herein mg#) in a range of 0.36 - 0.45, signifying that the studied basaltic samples do not represent a primary magma derived from partial melting of a normal mantle (Irving and Green, 1976; Frey *et al.*, 1978; Wilson, 1989). The nature of evolved basalt is in agreement with the relatively low concentrations of Ni (79 – 176 ppm, 139 ± 27 ppm on average) and Cr (207 – 369 ppm, 331 ± 42 ppm on average) (Frey *et al.*, 1978; Wilson, 1989), and their Zr/TiO_2 values (0.009 – 0.013, 0.011 ± 0.001 on average) (Figure 4.2).

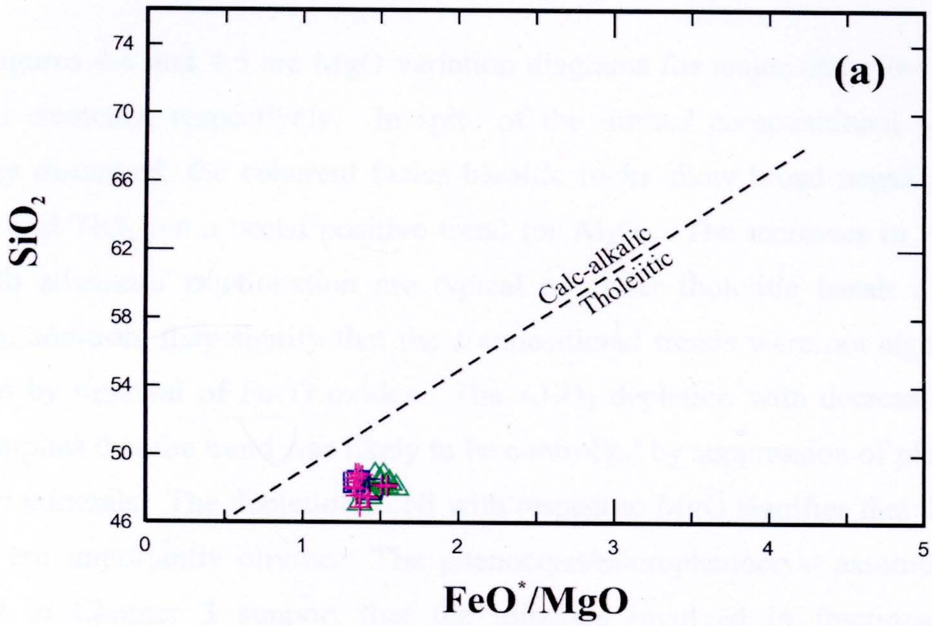

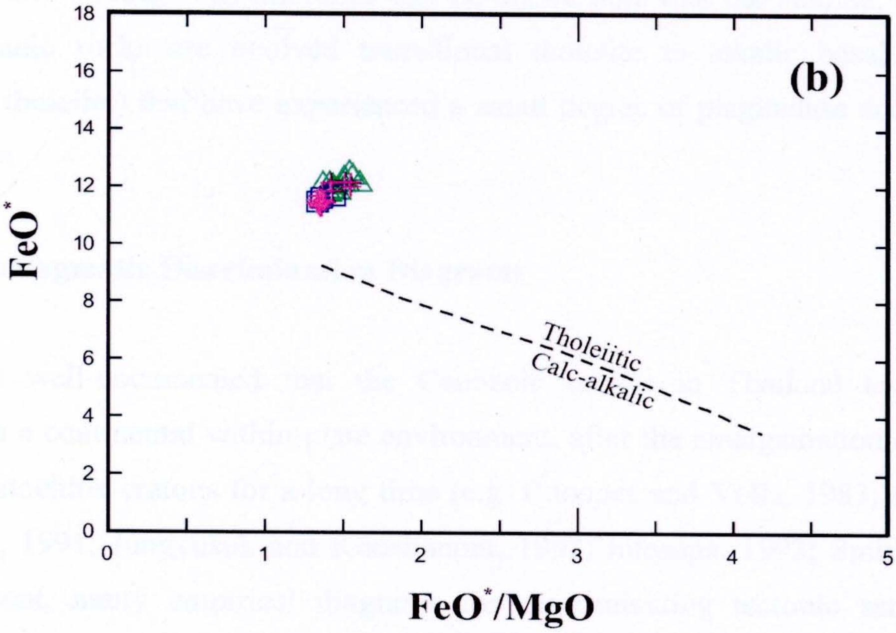

Figure 4.3 Plots of (a) SiO_2 and (b) FeO^* against FeO^*/MgO for the coherent facies basaltic rocks of the Ban Sap Sawat volcanic suite, Note that FeO^* denotes total iron as FeO, Field boundaries between tholeiitic and calc-alkalic fields are taken from Miyashiro (1975). Symbols are as in Figure 4.1.

Figures 4.4 and 4.5 are MgO variation diagrams for major and minor oxides, and trace elements, respectively. In spite of the limited compositional ranges as previously discussed, the coherent facies basaltic rocks show broad negative trends for FeO^* and TiO_2 but a broad positive trend for Al_2O_3. The increases in FeO^* and TiO_2 with advanced fractionation are typical of either tholeiitic basalt or alkalic basalt. In addition, they signify that the compositional trends were not significantly controlled by removal of Fe-Ti oxides. The Al_2O_3 depletion with decreasing MgO content implies that the trend was likely to be controlled by suppression of plagioclase and mafic minerals. The depletion in Ni with respect to MgO signifies that the mafic minerals are importantly olivine. The phenocryst/microphenocryst assemblages as discussed in Chapter 3 support that the minerals involved in fractionation are plagioclase and olivine. An inference can be drawn here that the studied, coherent facies volcanic rocks are evolved transitional tholeiite to alkalic basalt (herein transitional tholeiite) that have experienced a small degree of plagioclase and olivine fractionation.

4.4 Tectonomagmatic Discrimination Diagrams

It is well-documented that the Cenozoic basalts in Thailand have been generated in a continental within-plate environment, after the amalgamation of Shan-Thai and Indochina cratons for a long time (e.g. Bunopas and Vella, 1983; Barr and MacDonald, 1991; Jungyusuk and Khositanont, 1992; Intasopa, 1993; Smith 1996). Up to present, many empirical diagrams for discriminating tectonic settings of eruption have appeared in literature (e.g. Pearce and Cann, 1973; Pearce and Norry, 1979; Pearce, 1980, 1982; Shervais, 1982; Meschede, 1986).

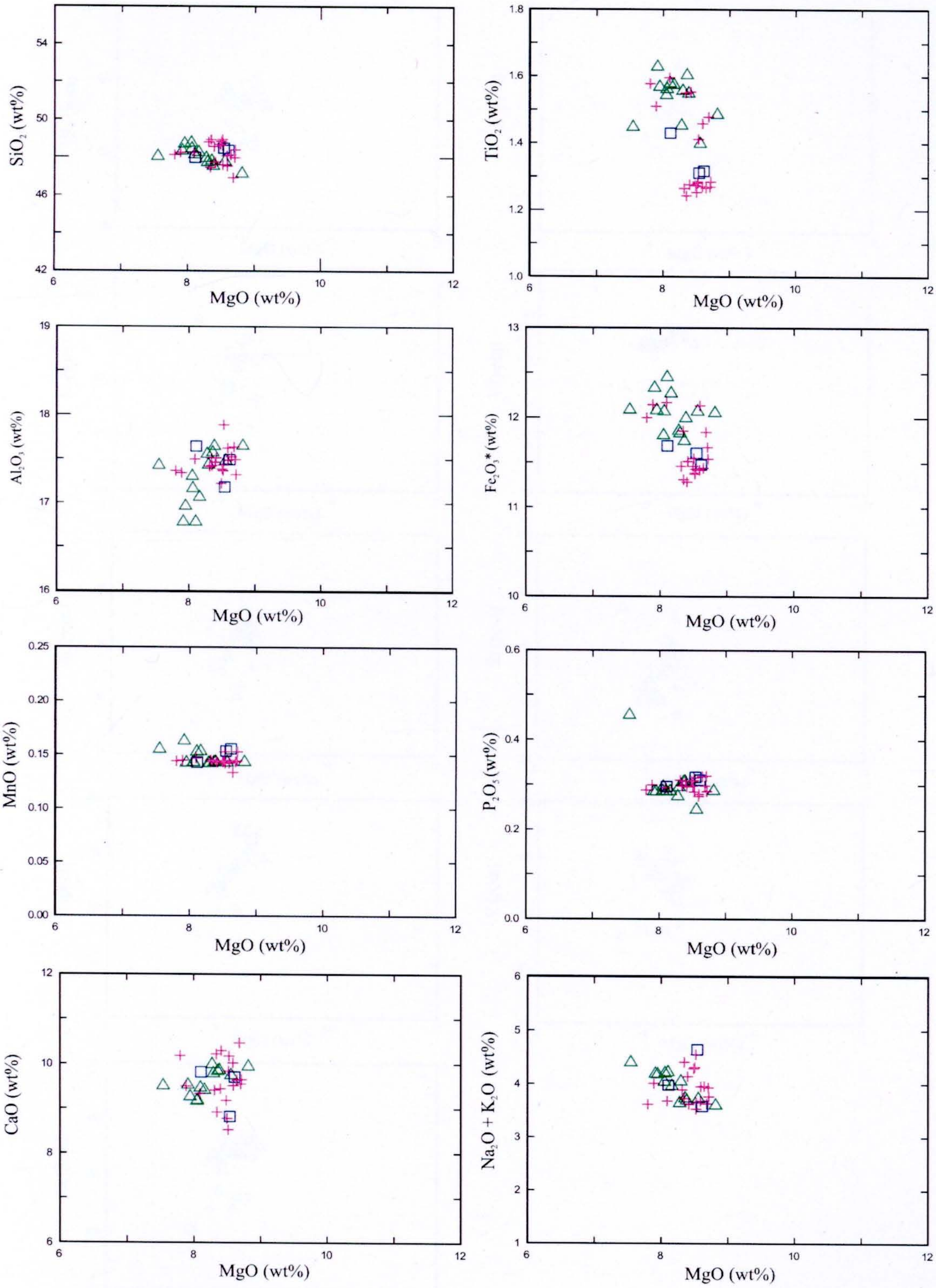

Figure 4.4 MgO variation diagrams for SiO_2, TiO_2, Al_2O_3, total iron as Fe_2O_3 ($Fe_2O_3^*$), MnO, P_2O_5, CaO and Na_2O+K_2O in the Ban Sap Sawat coherent facies basaltic rocks, Symbols are as in Figure 4.1.

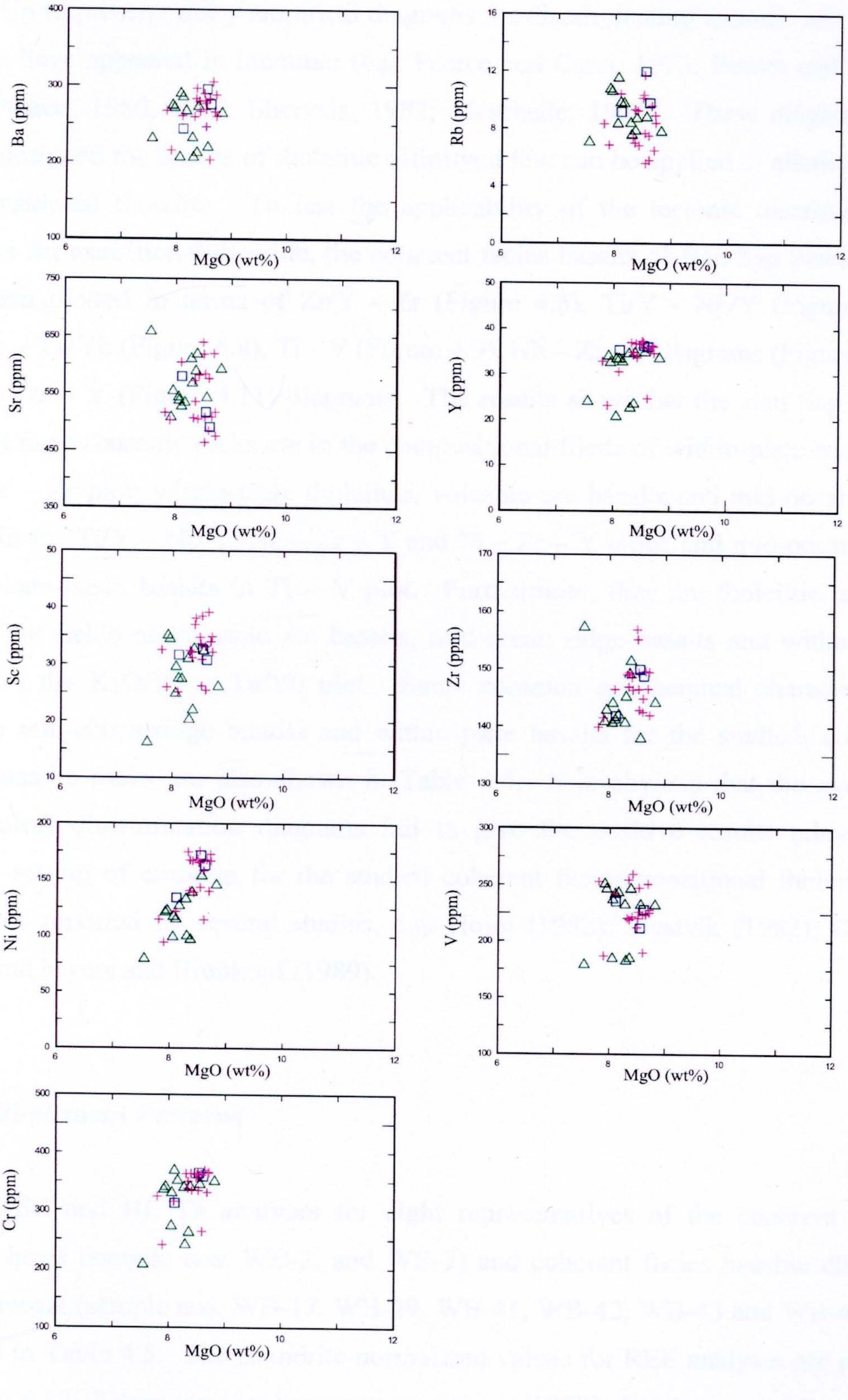

Figure 4.5 MgO variation diagrams for Ba, Rb, Sr, Y, Sc, Zr, Ni, V and Cr in the Ban Sap Sawat coherent facies basaltic rocks, Symbols are as in Figure 4.1.

Up to present, many empirical diagrams for discriminating tectonic settings of eruption have appeared in literature (e.g. Pearce and Cann, 1973; Pearce and Norry, 1979; Pearce, 1980, 1982; Shervais, 1982; Meschede, 1986). These diagrams are largely designed for basalts of tholeiitic affinity; a few can be applied to alkalic basalt and transitional tholeiite. To test the applicability of the tectonic discrimination diagrams for transitional tholeiite, the coherent facies basalts of Ban Sap Sawat suite have been plotted in terms of Zr/Y - Zr (Figure 4.6), Ti/Y - Nb/Y (Figure 4.7), K_2O/Yb – Ta/Yb (Figure 4.8), Ti - V (Figure 4.9), Nb – Zr - Y diagrams (Figure 4.10) and Ti – Zr - Y (Figure 4.11) diagrams. The results show that the Ban Sap Sawat coherent facies basaltic rocks are in the compositional fileds of within-plate basalts in the Zr/Y – Zr plot; within-plate tholeiites, volcanic arc basalts and mid-ocean ridge basalts in the Ti/Y – Nb/Y, Nb – Zr – Y and Ti – Zr – Y plots; and mid-ocean ridge and backarc-basin basalts in Ti – V plot. Furthermore, they are tholeiitic, and lie outside the fields of volcanic arc basalts, mid-ocean ridge basalts and within-plate basalts in the K_2O/Yb – Ta/Yb plot. Some common geochemical characteristics between mid-ocean-ridge basalts and within-plate basalts for the studied, coherent facies basaltic rocks are also shown in Table 4.4. It is obvious that the available geochemical discrimination diagrams fail to give the positive results relevant to tectonic setting of eruption for the studied coherent facies transitional tholeiites as previously reported by several studies, e.g. Holm (1982), Prestvik (1982), Duncan (1987) and Myers and Breitkopf (1989).

4.5 Multi-element Patterns

REE and Hf, Ta analyses for eight representatives of the coherent facies basaltic lavas (sample nos. WB-2, and WB-7) and coherent facies basaltic clasts in basalt breccia (sample nos. WB-17, WB-29, WB-41, WB-42, WB-43 and WB-44) are reported in Table 4.5. The chondrite-normalized values for REE analyses are plotted in Figure 4.12. These samples have narrow ranges of REE abundances, i.e. the values for La and Yb are in ranges of 12.5-15.2 and 2.19-2.8, respectively. The chondrite-normalized REE patterns for these transitional tholeiites are slightly LREE - enriched,

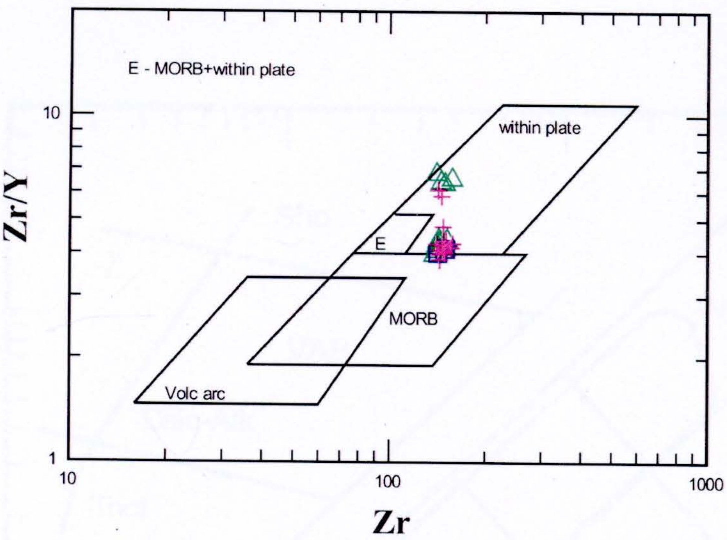

Figure 4.6 Plot of Zr/Y *versus* Zr for the coherent facies basaltic rocks presented in this study, The fields for within-plate basalts (WPB), volcanic arc basalts (VAB), mid-ocean ridge basalts (MORB), and within-plate basalts + mid-ocean ridge basalts (E) are taken from Pearce and Norry (1979). Symbols are as in Figure 4.1.

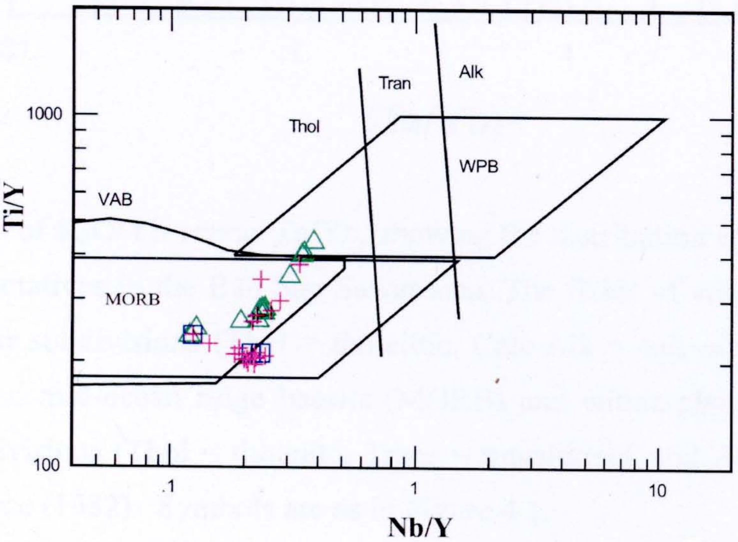

Figure 4.7 Ti/Y-Nb/Y tectonic discrimination diagram for the Ban Sap Sawat basaltic suite, The fields of within-plate basalts (WPB) and their subdivisions (Thol = tholeiitic, Trans = transitional, and Alk = alkalic), mid-ocean ridge basalts (MORB) and volcanic-arc basalt (VAB) are taken from Pearce (1982). Symbols are as in Figure 4.1.

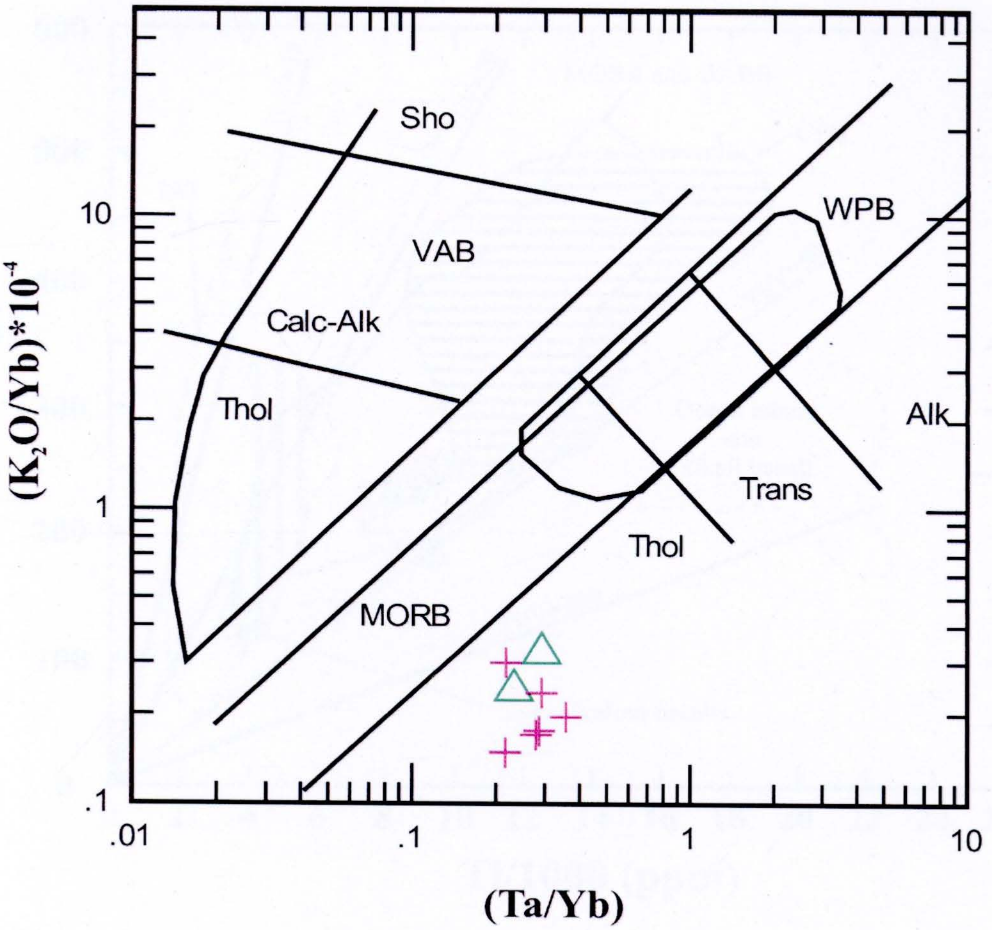

Figure 4.8 Plots of K_2O/Yb *versus* Ta/Yb, showing the distribution of coherent facies basaltic representatives in the Ban Sap Sawat area, The fields of volcanic-arc basalts (VAB) and their subdivisions (Thol = tholeiitic, Calc-Alk = calc-alkalic, and Sho = shoshonitic), and mid-ocean ridge basalts (MORB) and within-plate basalts (WPB) with their subdivisions (Thol = tholeiitc, Trans = transitional, and Alk = alkalic) are taken from Pearce (1982). Symbols are as in Figure 4.1.

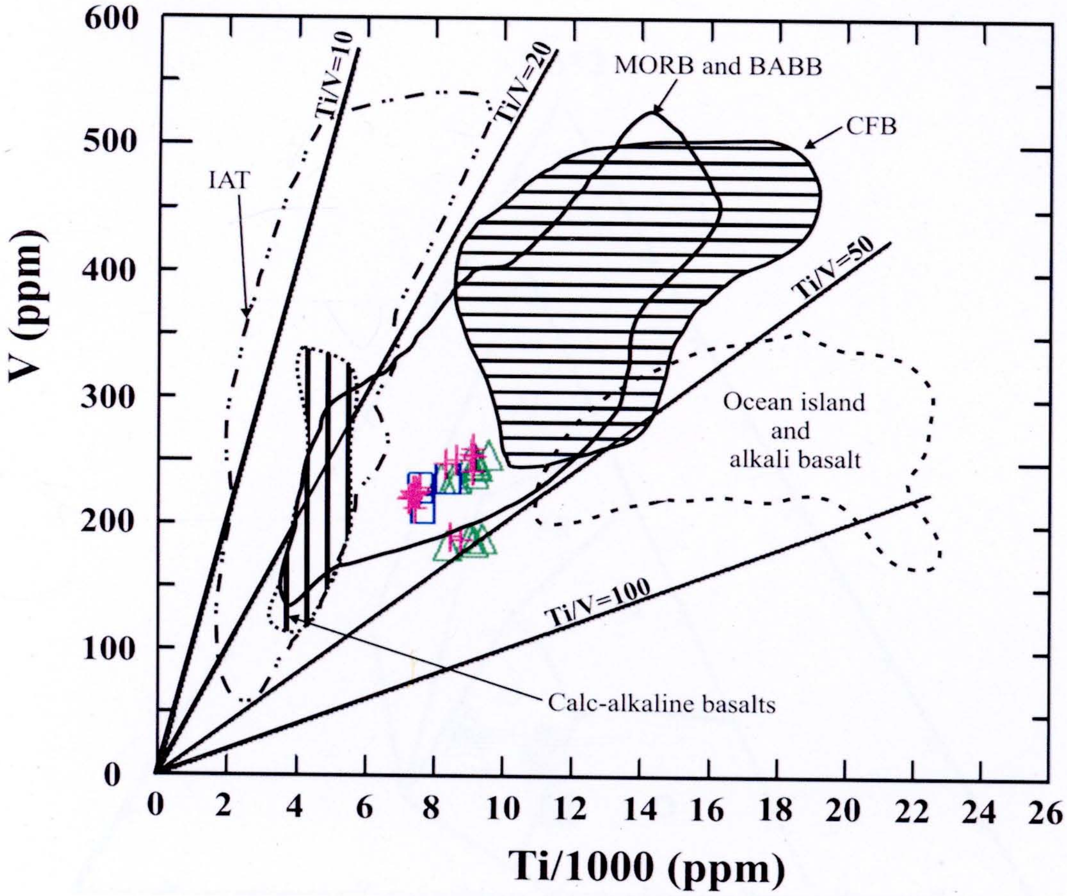

Figure 4.9 Tectonic discrimination diagram in terms of Ti and V (after Shervais, 1982) showing the distribution of Ban Sap Sawat coherent facies basaltic rocks, MORB = mid-ocean ridge basalt, BABB = back-arc basin basalt, IAT = island-arc tholeiite, and CFB = continental flood basalt, Symbols are as in Figure 4.1.

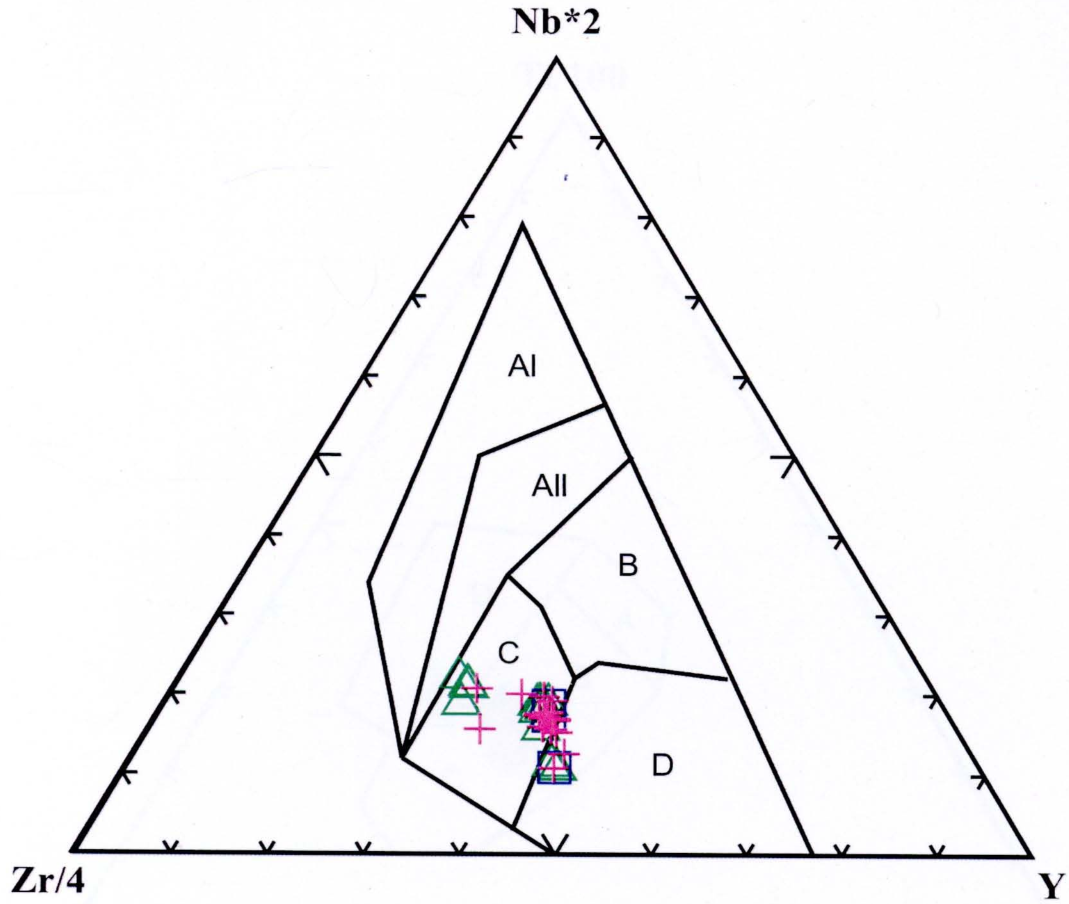

Figure 4.10 Nb-Zr-Y diagram for the Ban Sap Sawat coherent facies basaltic rocks, Also shown are the delimited fields for basalts of different tectonic environments (after Meschede, 1986). AI = within-plate alkalic basalt, AII = within-plate alkalic and tholeiitic basalt, B = E-MORB (enriched mid-ocean ridge basalt), C = within-plate tholeiitic basalt and volcanic arc basalt, and D = N-MORB (normal mid-ocean ridge basalt) and volcanic arc basalt. Symbols are as in Figure 4.1.

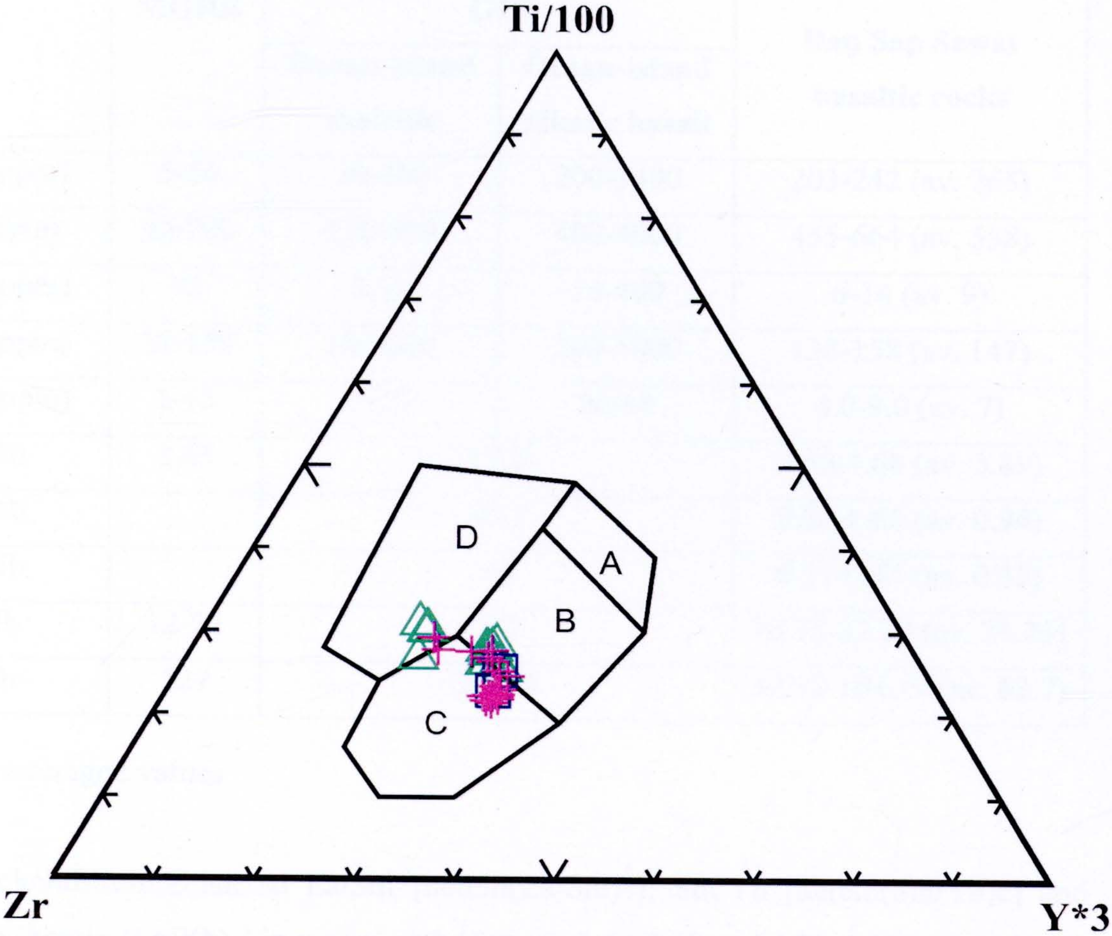

Figure 4.11 Ti-Zr-Y discrimination diagram (after Pearce and Cann, 1973) for the Ban Sap Sawat coherent facies basaltic rocks, A is the field of island-arc tholeiites, B = MORB, island-arc tholeiites and calc-alkali basalts, C = calc-alkali basalts, and D = within-plate basalts. Symbols are as in Figure 4.1.

Table 4.4 Comparison of the geochemical data for the Ban Sap Sawat coherent facies basaltic rocks, with those for mid–ocean island basalts (MORB) and ocean-island basalts (OIB) (data taken from Wilson, 1989).

	MORB	OIB		Ban Sap Sawat basaltic rocks
		Ocean-island tholeiite	Ocean-island alkalic basalt	
Ba (ppm)	5-50	70-200	200-1400	203-242 (av. 265)
Sr (ppm)	90-200	150-400	400-4000	455-664 (av. 558)
Rb (ppm)	<5	5-12	15-400	6-14 (av. 9)
Zr (ppm)	15-150	100-300	200-1000	138-158 (av. 147)
Nb (ppm)	1-15	5-25	20-60	4.0-9.0 (av. 7)
Ce/Nb	3.85	17.8		3.50-4.68 (av. 3.89)
Th/Nb		<0.1		0.50-1.65 (av. 0.94)
Hf/Nb		<8		0.31-0.45 (av. 0.35)
Zr/Nb	12-22	5.8		16.75-33.20 (av. 21.25)
Sr/Rb	127	20-70		39.58-104.19 (av. 62.7)

av = averaged values

with chondrite-normalized La/Sm [herein(La/Sm)c], Sm/Yb [herein(Sm/Yb)c] and La/Yb [herein $(La/Yb)_n$] in ranges of 2.19-2.68, 1.44-2.13 and 4.79-6.16, respectively. These patterns are typical of within-plate tholeiites, transitional tholeiites and enriched mid-ocean ridge basalts.

The N-MORB normalized patterns for the representatives of coherent facies basaltic rocks show a step-like patterns, with strong Sr, K, Rb, Ba and Th enrichment and Ta – Nb troughs (Figure 4.13). The Ta – Nb troughs rule out an oceanic within-plate environment. Accordingly, the Ban Sap Sawat transitional tholeiites have been erupted in a continental within-plate environment as expected.

Table 4.5 Rare-earth-element, Hf and Ta analyses (in ppm), and chondrite-normalized La/Yb, La/Sm and Sm/Yb of the representative Ban Sap Sawat coherent facies basaltic samples. The chondrite normalizing values used are those of Taylor and Gorton (1977).

	Sample No.							
	WB 2	WB 7	WB 17	WB 29	WB 41	WB 42	WB 43	WB 44
La	12.5	13.5	13.8	15.2	13.0	13.0	14.7	13.4
Ce	28.0	29.0	30.3	30.1	28.2	28.9	30.5	28.9
Pr	3.40	3.70	3.50	3.40	3.40	3.50	3.80	3.50
Nd	16.0	17.7	16.3	16.9	17.3	18.9	18.7	16.5
Sm	4.37	4.35	4.16	3.94	3.96	4.85	4.47	4.07
Eu	1.32	1.38	1.12	1.24	1.44	1.45	1.34	1.31
Gd	3.71	4.14	4.06	3.67	3.84	4.07	4.19	4.43
Tb	0.76	0.77	0.77	0.74	0.87	0.76	0.74	0.75
Dy	4.20	4.02	4.14	3.99	4.14	4.49	4.39	4.22
Ho	0.83	0.86	0.91	0.77	0.78	0.91	0.87	0.89
Er	2.32	2.39	2.45	2.48	2.15	2.29	2.28	2.46
Tm	0.34	0.34	0.36	0.38	0.29	0.37	0.40	0.35
Yb	2.19	2.19	2.88	2.68	2.48	2.28	2.45	2.32
Hf	2.45	2.56	2.71	2.49	2.61	2.67	2.76	2.77
Ta	0.64	0.51	0.62	0.58	0.72	0.81	0.68	0.66
La/Yb	5.70	6.16	4.79	5.67	5.24	5.70	6.00	5.77
La/Sm	2.86	3.10	3.32	3.86	3.28	2.68	3.29	3.29
Sm/Yb	2.00	1.99	1.44	1.47	1.60	2.13	1.82	1.75

Comparisons with modern lavas of different tectonic settings have been extensively carried out. The results, in terms of REE and N-MORB normalized multi-elements patterns (Figures 4.12 and 4.13) show that the Ban Sap Sawat transitional tholetiitic rocks are closely analogous to the Early-Middle Miocene, Central Sinkhote-Alin and Sakhalin basalts from northeastern margin of the Eurasian continent (Okamura *et al.*, 2005), which were erupted in a continental rift environment.

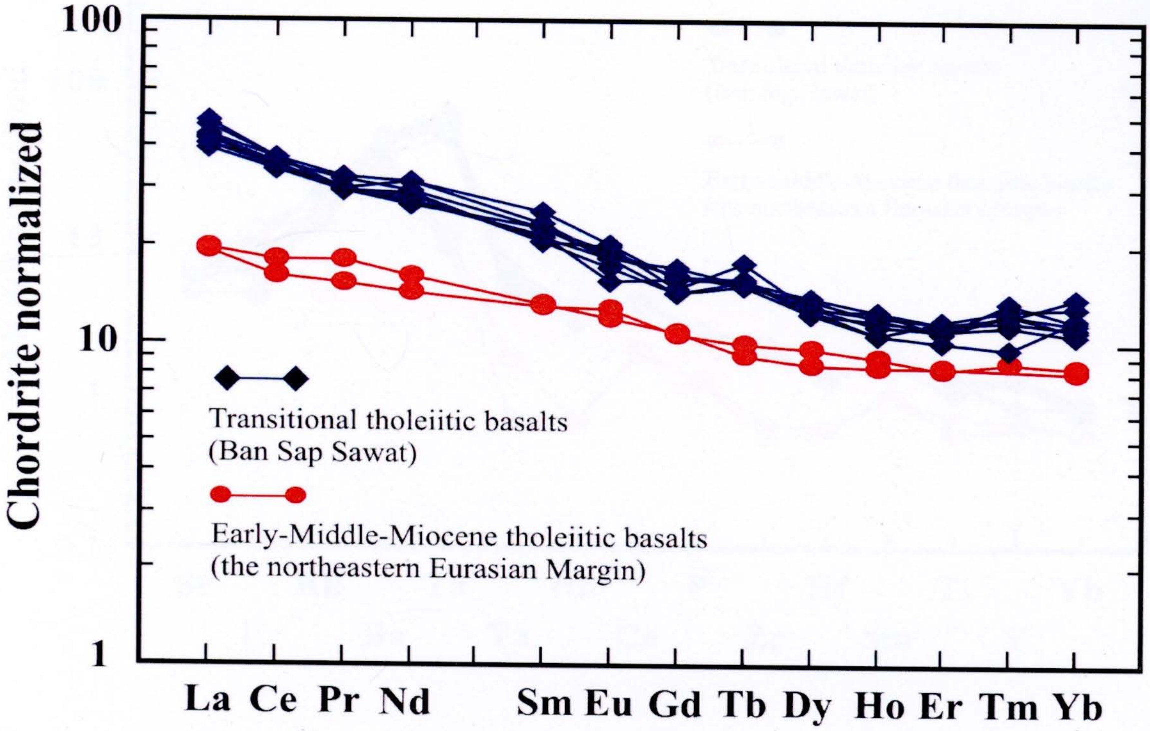

Figure 4.12 Chondrite-normalized REE patterns for the representative Ban Sap Sawat transitional tholeiitic basalts compared with those of Early-Middle Miocene, Central Sinkhote-Alin and Sakhalin tholeiitic basalts from the northeastern margin of the Eurasian continent (Okamura *et al.*, 2005). Normalizing values used are those of Taylor and Gorton (1977).

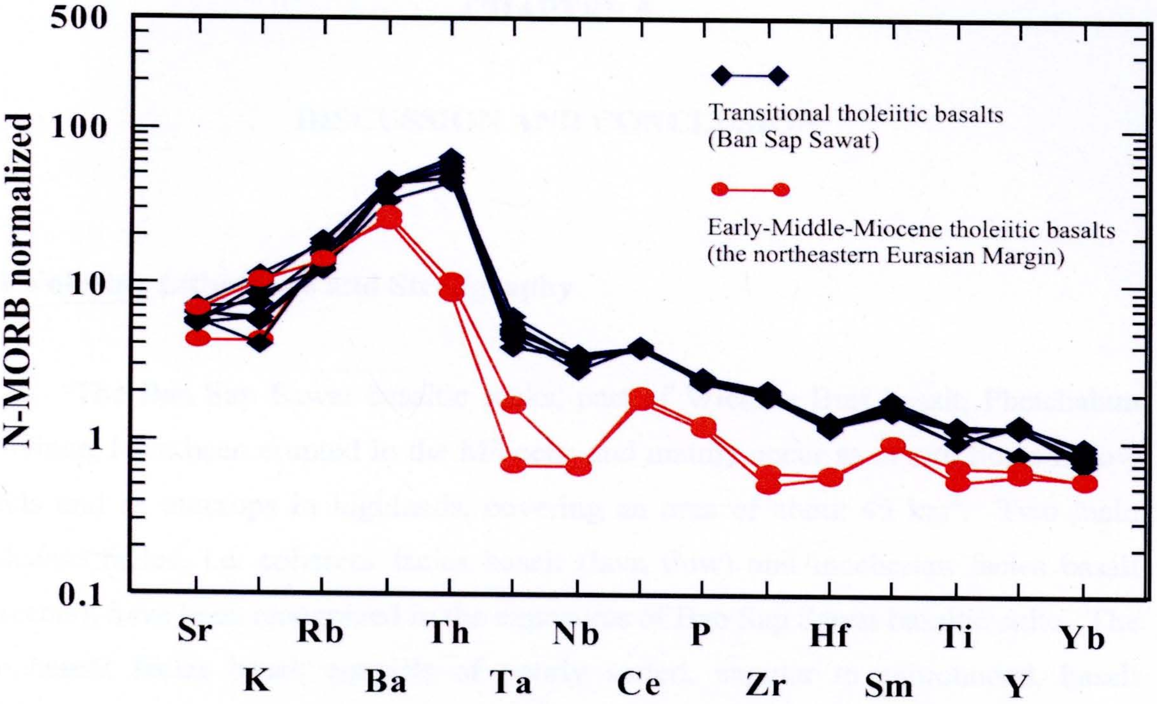

Figure 4.13 N-MORB normalized multi-element diagram of Pearce (1982, 1983) displaying the patterns for eight representative Ban Sap Sawat transitional tholeiitic basalts compared with those of the Early-Middle Miocene, Central Sinkhote-Alin and Sakhalin tholeiitic basalts from the northeastern margin of the Eurasian continent (Okamura *et al.*, 2005). N-MORB normalizing values used are those of Sun and McDonough (1989).